



Distinguishing and controlling Mottness in 1T-TaS₂ by ultrafast lightChanghua Bao,¹ Haoyuan Zhong,¹ Fei Wang,¹ Tianyun Lin,¹ Haoxiong Zhang,¹ Zhiyuan Sun,¹
Wenhui Duan ^{1,2} and Shuyun Zhou ^{1,2,*}¹State Key Laboratory of Low-Dimensional Quantum Physics and Department of Physics, Tsinghua University,
Beijing 100084, People's Republic of China²Frontier Science Center for Quantum Information, Beijing 100084, People's Republic of China

(Received 3 November 2022; revised 23 February 2023; accepted 27 February 2023; published 15 March 2023)

Distinguishing and controlling the extent of Mottness is important for materials where the energy scales of the on-site Coulomb repulsion U and the bandwidth W are comparable. Here, we report the ultrafast electronic dynamics of 1T-TaS₂ by ultrafast time- and angle-resolved photoemission spectroscopy. A comparison of the electron dynamics for the intermediate phase (I-phase) as well as the low-temperature commensurate charge density wave (C-CDW) phase shows distinctive dynamics. While the I-phase is characterized by an instantaneous response and nearly time-resolution-limited fast relaxation (~ 200 fs), the C-CDW phase shows a delayed response and a slower relaxation (a few ps). Such distinctive dynamics reflect the different relaxation mechanisms and provide nonequilibrium signatures to distinguish the Mott insulating I-phase from the C-CDW band insulating phase. Moreover, a light-induced bandwidth reduction is observed in the C-CDW phase, pushing it toward the Mott insulating phase. Our work demonstrates the power of an ultrafast light-matter interaction in both distinguishing and controlling the extent of Mottness on the ultrafast timescale.

DOI: [10.1103/PhysRevB.107.L121103](https://doi.org/10.1103/PhysRevB.107.L121103)

In condensed matter physics, the effect of an electron-electron (el-el) correlation strongly depends on the relative energy scales of the on-site Coulomb repulsion U and the bandwidth W [1,2]. When $W \gg U$, the physics is dominated by electron hopping as well as an electron-phonon (el-ph) interaction [Fig. 1(a)]. In contrast, when $W \ll U$, the el-el correlation plays a critical role, which forbids double occupancy of electrons on a single site. This results in a Mott insulating state even at half filling [Fig. 1(b)], which could lead to exotic electronic states such as unconventional superconductivity upon doping [3,4]. However, for insulators with comparable W and U [Fig. 1(c)], it is difficult to experimentally determine whether it is a Mott insulator from measurements in the equilibrium state. Finding an effective pathway to distinguish and further control the extent of Mottness in the nonequilibrium state is therefore important.

Ultrafast pump-probe measurements provide opportunities for distinguishing the different types of insulators via their dynamics relaxation upon photoexcitation [5,6]. For band insulators, the nonequilibrium electronic dynamics typically involves a slow interband relaxation through radiation recombination, Auger recombination, and carrier diffusion, etc. [7]. In contrast, the electronic dynamics of Mott insulators is somewhat faster through an el-el interaction [8–14]. For example, the photoexcitation of the Mott insulator VO₂ leads to an instantaneous modification of the electronic correlation and collapse of the band gap [11], and an ultrafast reduction of the Coulomb interaction is also expected for NiO [13]. In addition, a fast relaxation via annihilation of the dou-

blon (double-carrier occupancy on a single site) and holon (no carrier occupancy) through electron hopping [9,10], as schematically illustrated in Fig. 1(e), has also been reported for cuprates [8], ET-F₂TCNQ [12], and Ca₂RuO₄ [14]. Moreover, the comparable energy scales also make the material particularly sensitive to external perturbations such as ultrafast laser excitation [15], and therefore the light-matter interaction can also be potentially used as a control knob for tailoring the electronic structure by renormalizing U [16,17] or W .

Transition-metal dichalcogenide 1T-TaS₂ is a model material with similar energy scales of W and U . It shows rich charge density wave (CDW) phases at low temperatures [18,19], which folds the bands into a smaller Brillouin zone and reduces W to be comparable to the effective U [20–24]. Over the past few decades, the low-temperature commensurate CDW (C-CDW) phase had been considered as a Mott insulator because of the insulating behavior at half filling [21,25–28]. However, recent experimental results suggest that the C-CDW phase shows a large bandwidth [29–31], which originates from the layer dimerization [31–35] and stacking order [34,36–40] [Fig. 1(d)]. The dimerization leads to unit cell doubling with two electrons occupying each unit cell (full band filling), suggesting that the C-CDW phase is likely a band insulator, although some extent of correlation or Mottness may also exist. More importantly, an intermediate phase (I-phase) has been recently reported upon heating from the C-CDW phase into the triclinic CDW (T-CDW) phase [31]. The I-phase shows a significantly reduced bandwidth, and the filling is reduced by half due to the removal of the layer dimerization [Fig. 1(e)], and thereby it has been proposed to be a true Mott insulator.

Ultrafast time- and angle-resolved photoemission spectroscopy (Tr-ARPES) is a powerful technique for revealing

*Author to whom correspondence should be addressed: syzhou@mail.tsinghua.edu.cn

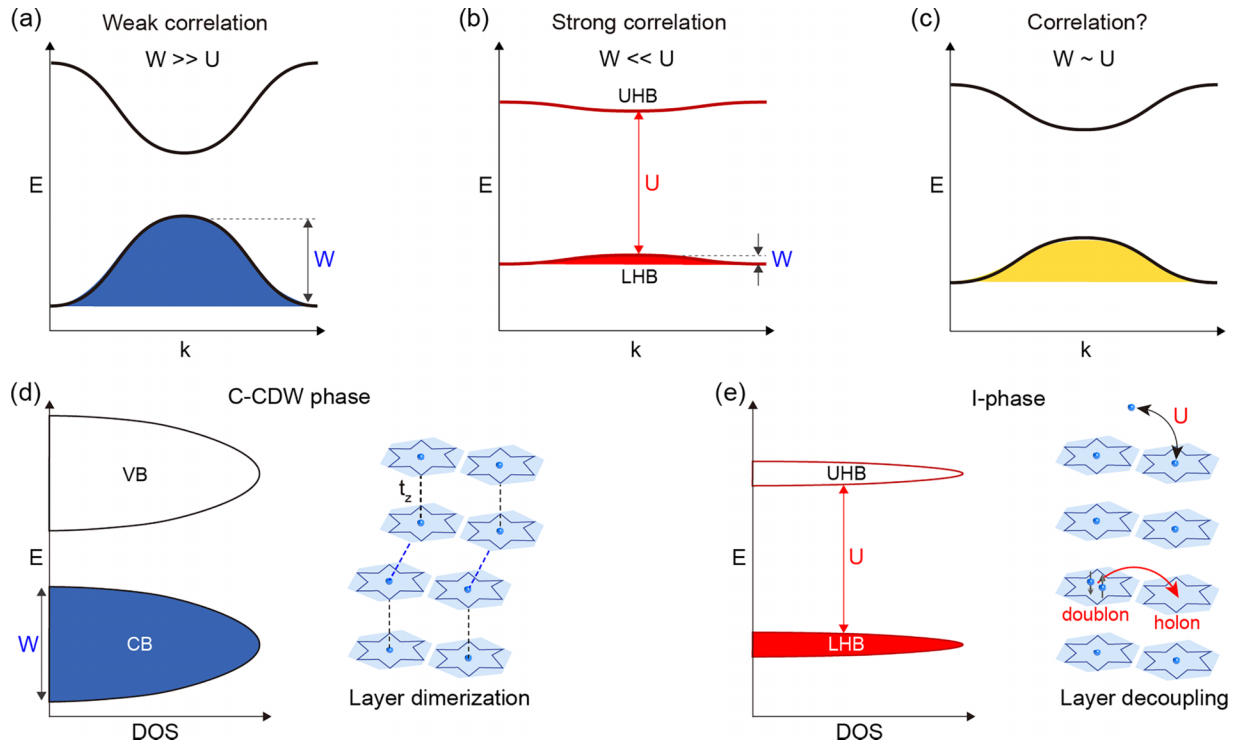


FIG. 1. Classification of weak, strong, and intermediate correlations according to the relative energy scales of W and U . (a)–(c) Schematic dispersions for weak, strong, and intermediate correlations according to the relative energy scales of W and U . (d) Schematics for the energy diagram and layer dimerization in the C-CDW phase of $1T$ -TaS₂. (e) Schematics for the energy diagram and dominant interactions in the I-phase of $1T$ -TaS₂.

the different mechanisms underlying the ultrafast dynamics. While previous Tr-ARPES works on $1T$ -TaS₂ have reported the carrier dynamics of the C-CDW phase, the room-temperature metallic phase, and the pump-induced hidden phase [5,24,41–49], a report on the electronic dynamics of the I-phase is missing. Here, we report the ultrafast electronic dynamics of the I-phase and provide nonequilibrium dynamical signatures to support that the I-phase is a Mott insulator while the C-CDW phase is a band insulator. Moreover, a transient light-induced band flattening is observed in the C-CDW phase, pushing it toward the Mott insulating phase.

Figure 2 shows a comparison of the experimental electronic structures for the C-CDW phase and the proposed Mott insulating I-phase. The large-range dispersion image of the C-CDW phase shows no band crossing at the Fermi energy E_F in Fig. 2(a), in agreement with the insulating property from previous ARPES measurements [21,50] as well as resistivity measurements in Fig. 2(d). Figures 2(b) and 2(c) show a comparison of the zoom-in dispersion images near the Γ point with a high-resolution laser source for both the C-CDW phase and I-phase. The comparison shows that the band near E_F has a larger bandwidth and band broadening in the C-CDW phase [Fig. 2(b)], while the bandwidth is significantly reduced in the I-phase [Fig. 2(c)], which is in agreement with the proposed Mott insulating phase by a recent synchrotron-based ARPES study [31]. The reduction of the bandwidth is more clearly observed from a comparison of the extracted dispersions shown in Fig. 2(e) (Fig. S1 [51]). In particular, upon a transition from the C-CDW phase to I-phase, the dispersion near the Γ point shifts down while the dispersion at the momenta away

from the Γ point shifts up. Such a reduction of the bandwidth increases the extent of Mottness in the equilibrium state of the I-phase. In addition, it shows that the electronic structure near Γ is more sensitive to the layer dimerization, while the electronic states away from Γ are much less sensitive.

To reveal the nonequilibrium dynamics of these two phases in the time domain, Tr-ARPES measurements have been performed with a weak pump of 0.3 mJ/cm^2 to avoid the pump-induced hidden phase [52,53]. We first focus on the electronic dynamics in the C-CDW phase [Fig. 3(a)]. A comparison of the energy distribution curves (EDCs) at the Γ point before and after pumping shows that the peak position moves down in energy by 20 meV upon pumping in Fig. 3(b), indicating a light-induced band shift ΔE as represented by the red arrow in Fig. 3(b). In addition, the intensity also decreases upon pumping as represented by the blue area in Fig. 3(b), suggesting the emergence of photoexcited holes. Therefore, the change in the intensity can be used to represent the amount of photoexcited holes (Δn).

Figure 3(c) shows the continuous evolution of the EDCs with delay time, where clear oscillations in the peak position and peak intensity are observed. The extracted photoexcited carrier density Δn and light-induced band shift ΔE are shown in Figs. 3(d) and 3(e), both of which show an oscillating behavior with a period of 410 fs (2.44 THz from the Fourier transformation shown in Fig. S2 [51]) due to the CDW amplitude mode [41]. Here, we focus on the nonoscillating part including excitation (buildup) time as well as the relaxation time to search for signatures to distinguish the Mottness. First of all, Δn shows a buildup time of 0.2 ps , which is comparable

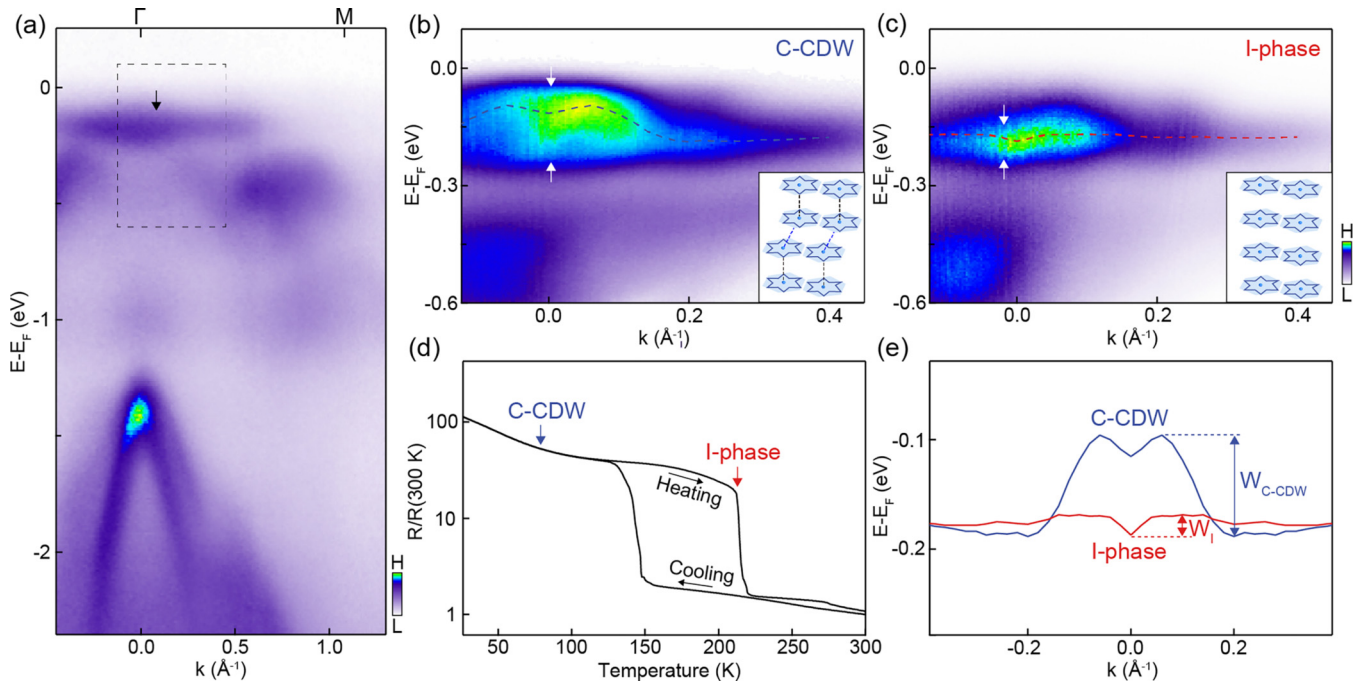


FIG. 2. A comparison of the experimental electronic structures for C-CDW phase and I-phase. (a) Dispersion image of C-CDW phase by using a helium lamp source at 80 K. (b), (c) Zoom-in dispersion images measured near the Γ point [marked by a dashed rectangle in (a)] by using a high-resolution laser source for (b) the C-CDW phase at 80 K and (c) the I-phase at 210 K upon heating. The insets are corresponding schematic crystal structures. (d) Normalized resistance as a function of temperature. (e) A comparison of dispersions extracted from the data shown in (b) and (c). The dispersions are symmetrized with respect to the Γ point.

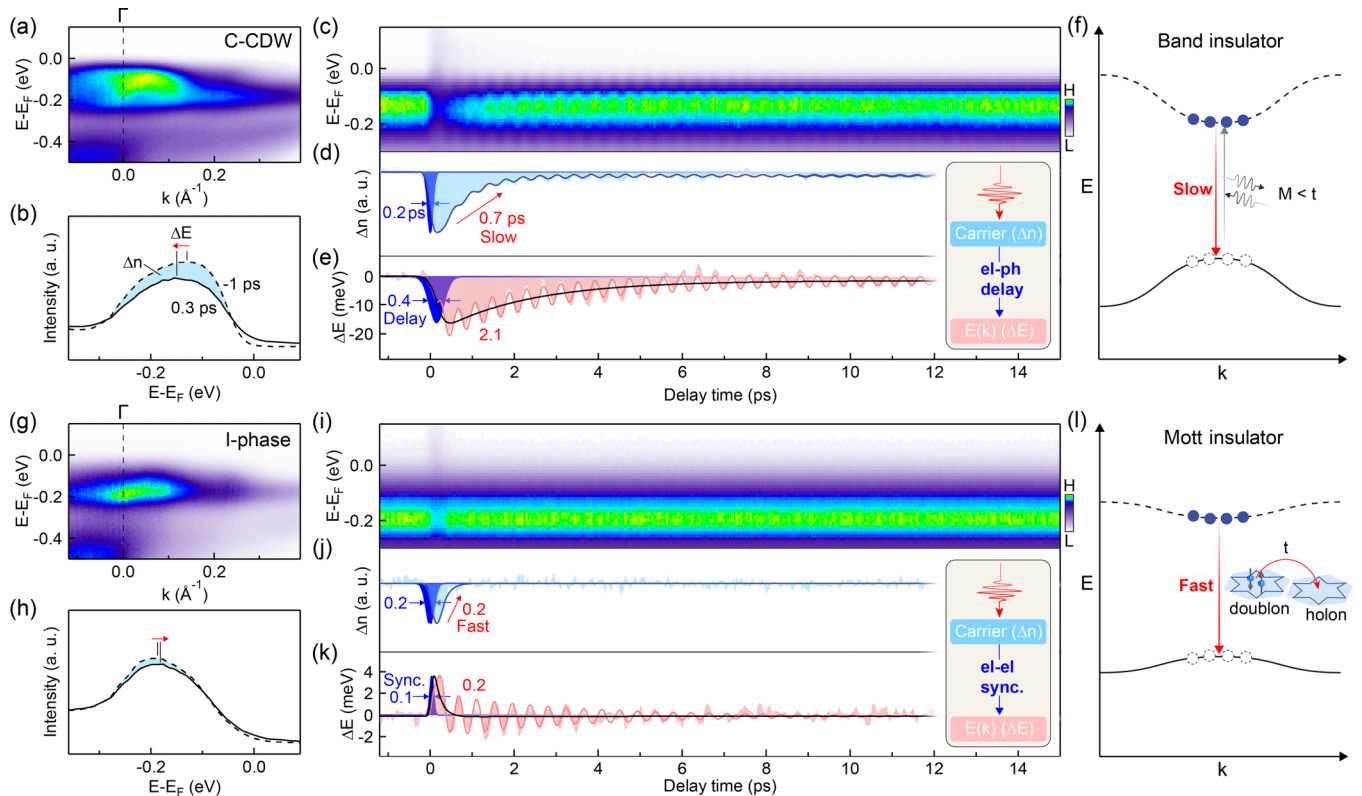


FIG. 3. Distinguishing Motttness in the electronic dynamics. (a) Dispersion image of the C-CDW phase at 80 K before pumping. (b) EDCs at the Γ point measured at $\Delta t = -1$ and 0.3 ps. (c) Evolution of EDCs at the Γ point as a function of delay time. (d), (e) Extracted photocarrier density Δn and band shift ΔE as a function of delay time. (f) A schematic of the slow relaxation in the C-CDW phase through radiation and reabsorption of photons. (g)–(k) Similar data to (a)–(e) for the I-phase measured at 210 K. (l) A schematic of the fast relaxation in the I-phase, which corresponds to the annihilation of a doublon and a holon.

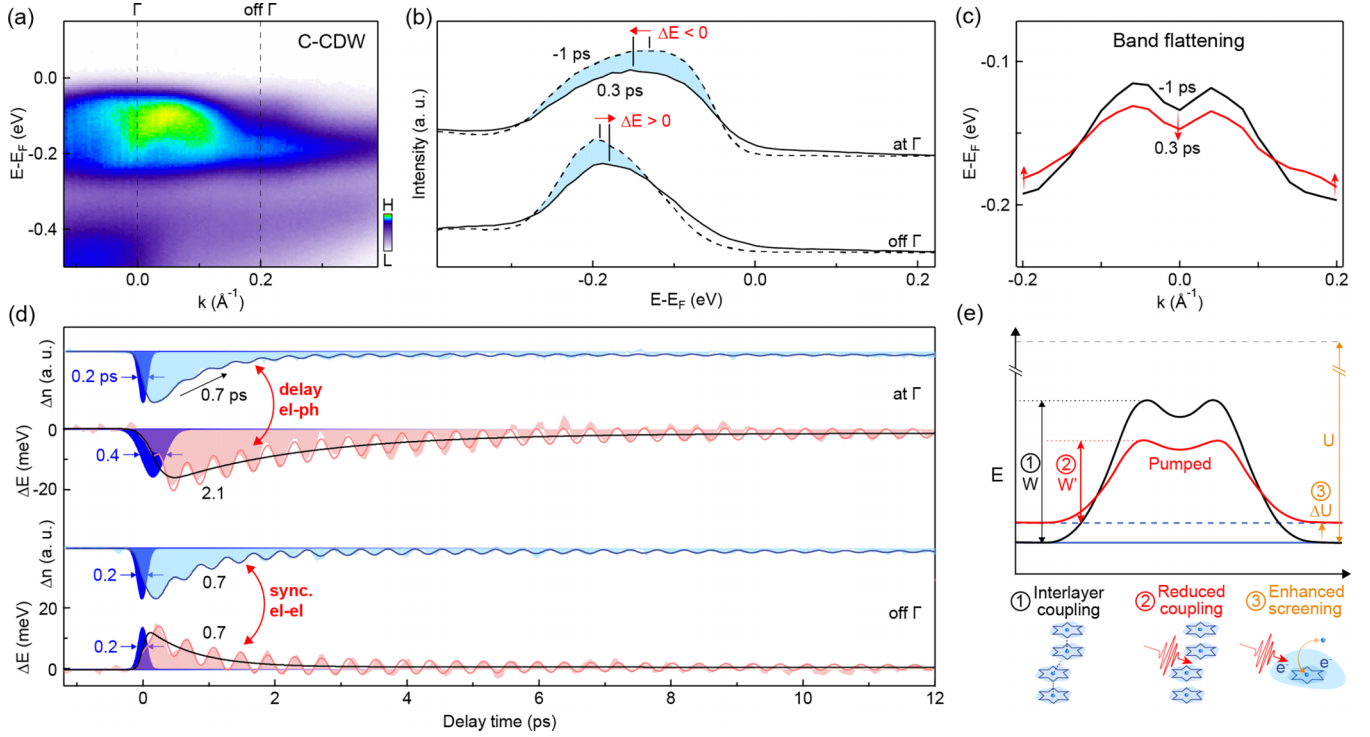


FIG. 4. Light-induced band flattening in the C-CDW phase. (a) Dispersion image of the C-CDW phase. (b) EDCs at Γ and off the Γ point [marked by dashed lines in (a)] at $\Delta t = -1$ and 0.3 ps. (c) Extracted dispersions at $\Delta t = -1$ and 0.3 ps. (d) Extracted band shift ΔE and photoexcited carrier density Δn as a function of delay time for Γ and off the Γ point. (e) A schematic summary of the origin of momentum-dependent dynamics.

to the experimental time resolution of 0.16 ps, while ΔE shows a slower buildup time of 0.4 ps. The delayed response between ΔE and Δn is consistent with the timescale of the el-ph interaction in $1T$ -TaS₂ [54], suggesting that the evolution of the electronic band likely involves the el-ph interaction as illustrated in the inset of Fig. 3(d), and thus that the C-CDW phase is a band insulator. Second, the relaxation also gives some hints for the band insulator. In particular, Δn shows a relaxation time of 0.7 ps with many periods of oscillation. One mechanism for this slow relaxation is through interband decay channels [7] such as electron-hole recombination by the emission of phonons or photons, as schematically illustrated in Fig. 3(f), which is typical for a band insulator. This process is slow because of the weak interband matrix element M of the electron-boson interaction. The second possibility is that the relaxation comes from the recovery of the pump-suppressed interlayer CDW order (the layer dimerization), which is slow due to the involvement of the lattice degrees of freedom. We note that although the C-CDW phase seems to be a band insulator from the point of view in the time domain, some extent of correlation such as the Mottness may also exist, for example, a short-lived upper Hubbard band has been reported in some specific $1T$ -TaS₂ samples [24].

In contrast to the C-CDW phase, the dynamics in the I-phase [Fig. 3(g)] is very different. The EDC analysis in Figs. 3(h) and 3(i) shows a much weaker response upon pumping at the same pump fluence. Although the oscillation period of 430 fs (2.36 THz from the Fourier transformation in Fig. S2 [51]) is overall similar to the C-CDW phase, both the buildup and relaxation time are faster than those in the

C-CDW phase. First, upon pumping, both Δn and ΔE show a nearly resolution-limited response within 0.1–0.2 ps, and they are simultaneous without any delayed response [Figs. 3(j) and 3(k)], suggesting the band shift occurs on a much faster timescale and is driven by photoexcited carriers through the el-el interaction, as illustrated in the inset of Fig. 3(j). Second, Δn relaxes within 0.2 ps, which is much faster than the 0.7 ps observed in the C-CDW phase. Such an ultrafast relaxation time is in line with the reported fast electronic relaxation in other Mott insulators [8,11,12,14,17,55] and suggests that the relaxation is driven by annihilation of doublons and holons which is featured in Mott insulators. As illustrated in Fig. 3(l), the interband relaxation in a Mott insulator is intrinsically distinct from a band insulator due to the strong el-el correlation and corresponds to an electron hopping process from a double-occupied site (doublon) to the unoccupied site (holon) with a fast recombination rate exponentially dependent on the ratio of Hubbard U to exchange energy J [9,10]. To summarize this part, the instantaneous band renormalization and photoexcited carriers with nearly time-resolution-limited excitation and relaxation times further support that the I-phase is a Mott insulating phase.

Such an ultrafast light-matter interaction can be used not only to distinguish the Mott insulating state, but also to control the extent of Mottness, which is supported by the observed light-induced band flattening in the C-CDW phase. The light-induced band shift is found to be strongly momentum dependent, in particular, the peak shifts down at the Γ point, while it shifts up at a momentum away from the Γ point, as shown in Fig. 4(b). The extracted dispersions before and

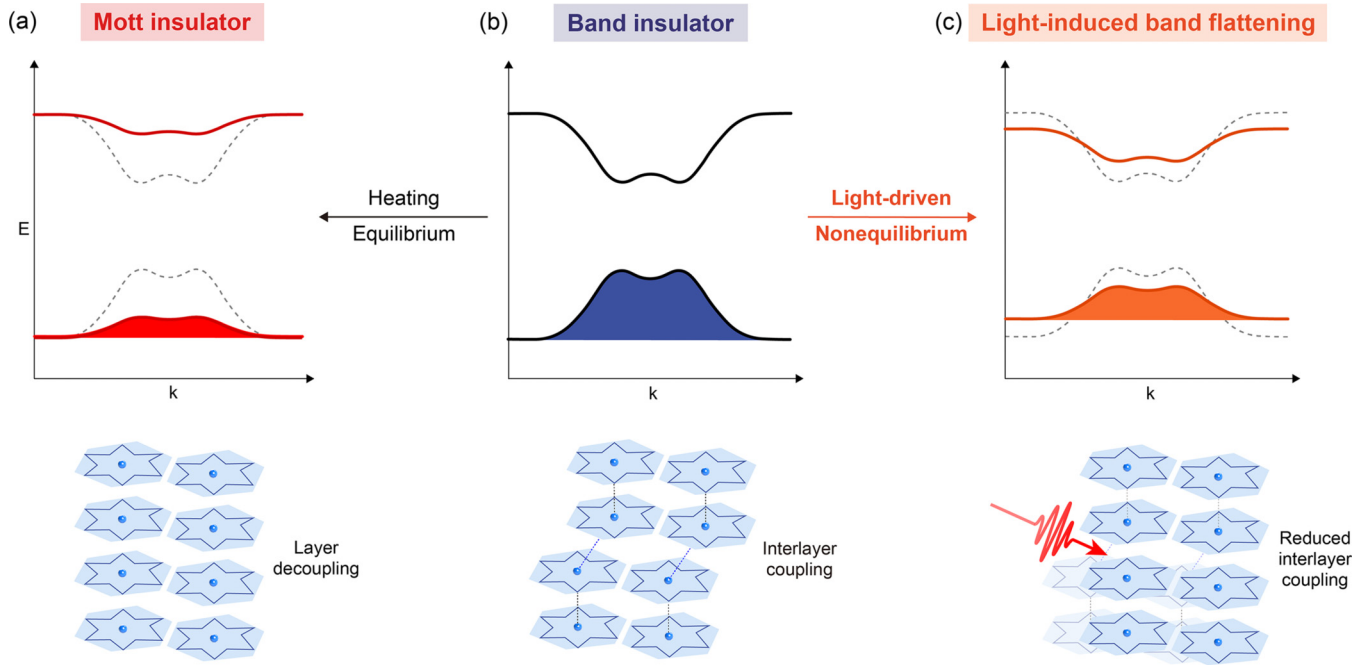


FIG. 5. Band flattening upon photoexcitation and heating. (a) Mott insulating phase induced by heating upon interlayer decoupling. (b) The band insulating phase with a dispersive band due to the interlayer coupling in the ground state. (c) The light-induced transient band flattening by reducing the interlayer coupling strength in the nonequilibrium state.

after pumping further show that the opposite movements of the bands at and off the Γ point lead to a reduction of the bandwidth from 80 to 50 meV, as shown in Fig. 4(c), demonstrating that ultrashort light pulses can be used to control the bandwidth, which is critical for determining the extent of Mottness. Here, the light-induced reduction of the bandwidth in the C-CDW phase pushes it toward the Mott insulating phase and increases the extent of Mottness.

To explore the underlying mechanism behind the exotic light-induced band flattening, Fig. 4(d) shows the evolution of the ΔE and Δn in the time domain both at and off the Γ point, and a clear momentum dependence is observed in the dynamics. First, compared to the delayed evolution between ΔE and Δn from el-ph coupling at the Γ point, they are synchronized off the Γ point, suggesting the band off the Γ point is dominated by the el-el interaction, in contrast to the I-phase where synchronized ΔE and Δn are observed both at Γ and off the Γ points (Fig. S3 [51]). Second, ΔE measured off the Γ point shows an opposite sign from that measured at the Γ point. This can be understood by the photodoping-induced screening as schematically illustrated in Fig. 4(e), which reduces U as reported in other correlated materials [13,16,17] and leads to an upward band shift. The downward energy shift at the Γ point can be understood by the reduction of W due to light-induced weakening of the interlayer coupling, which is supported by the disappearance of the interlayer dimerization at a higher pump fluence revealed by ultrafast x-ray and electron diffraction measurements [35,56] as well as a rearrangement of the stacking order suggested by optical measurements [57]. Although U is also reduced by the photodoping effect, W shows a much larger reduction and longer lifetime, thus still pushing the system towards the Mott insulating phase [51].

In summary, our Tr-ARPES measurements reveal the nearly time-resolution-limited excitation and ultrafast relaxation dynamics in the I-phase of $1T$ -TaS₂, in contrast to the delayed response and a slower relaxation in the C-CDW phase. Such different responses suggest that the I-phase is dominated by the el-el interaction, providing evidence for its Mott insulating nature from the nonequilibrium dynamics. In addition, owing to the unique energy, momentum, and time resolution of Tr-ARPES measurements, a light-induced momentum-dependent band flattening is revealed in the C-CDW phase. The observed light-induced tuning of the electronic structure toward the Mott insulating phase is complementary to the heating-induced Mott insulating phase in the equilibrium state, while extending the control of the electronic structure to the ps timescale, as schematically summarized in Fig. 5. The light-induced reduction of the bandwidth is likely associated with the suppression of the interlayer dimerization, which was indicated by ultrafast diffraction and optical measurements [35,56,57]. Our work demonstrates that ultrafast light pulses can be used not only to distinguish, but also to control the Mottness on the ultrafast timescale, which is particularly useful for systems with similar energy scales of W and U .

This work was supported by the National Key R&D Program of China (No. 2021YFA1400100), the National Natural Science Foundation of China (No. 12234011, No. 92250305, No. 11725418, and No. 11427903), and National Key R&D Program of China (No. 2020YFA0308800). C.B. is supported by a project funded by China Postdoctoral Science Foundation (No. 2022M721886) and the Shuimu Tsinghua Scholar Program.

The authors have no conflicts to disclose.

- [1] N. F. Mott, *Proc. Phys. Soc. A* **62**, 416 (1949).
- [2] M. Imada, A. Fujimori, and Y. Tokura, *Rev. Mod. Phys.* **70**, 1039 (1998).
- [3] A. Damascelli, Z. Hussain, and Z.-X. Shen, *Rev. Mod. Phys.* **75**, 473 (2003).
- [4] P. A. Lee, N. Nagaosa, and X.-G. Wen, *Rev. Mod. Phys.* **78**, 17 (2006).
- [5] S. Hellmann, T. Rohwer, M. Kalläne, K. Hanff, C. Sohr, A. Stange, A. Carr, M. Murnane, H. Kapteyn, L. Kipp *et al.*, *Nat. Commun.* **3**, 1069 (2012).
- [6] Y. Wang, B. Moritz, C.-C. Chen, C. J. Jia, M. van Veenendaal, and T. P. Devereaux, *Phys. Rev. Lett.* **116**, 086401 (2016).
- [7] S. Sundaram and E. Mazur, *Nat. Mater.* **1**, 217 (2002).
- [8] H. Okamoto, T. Miyagoe, K. Kobayashi, H. Uemura, H. Nishioka, H. Matsuzaki, A. Sawa, and Y. Tokura, *Phys. Rev. B* **82**, 060513(R) (2010).
- [9] N. Strohmaier, D. Greif, R. Jördens, L. Tarruell, H. Moritz, T. Esslinger, R. Sensarma, D. Pekker, E. Altman, and E. Demler, *Phys. Rev. Lett.* **104**, 080401 (2010).
- [10] Z. Lenarčič and P. Prelovšek, *Phys. Rev. Lett.* **111**, 016401 (2013).
- [11] D. Wegkamp, M. Herzog, L. Xian, M. Gatti, P. Cudazzo, C. L. McGahan, R. E. Marvel, R. F. Haglund, Jr., A. Rubio, M. Wolf *et al.*, *Phys. Rev. Lett.* **113**, 216401 (2014).
- [12] M. Mitrano, G. Cotugno, S. R. Clark, R. Singla, S. Kaiser, J. Stahler, R. Beyer, M. Dressel, L. Baldassarre, D. Nicoletti, A. Perucchi, T. Hasegawa, H. Okamoto, D. Jaksch, and A. Cavalleri, *Phys. Rev. Lett.* **112**, 117801 (2014).
- [13] N. Tancogne-Dejean, M. A. Sentef, and A. Rubio, *Phys. Rev. Lett.* **121**, 097402 (2018).
- [14] X. Li, H. Ning, O. Mehio, H. Zhao, M.-C. Lee, K. Kim, F. Nakamura, Y. Maeno, G. Cao, and D. Hsieh, *Phys. Rev. Lett.* **128**, 187402 (2022).
- [15] L. Stojchevska, I. Vaskivskiy, T. Mertelj, P. Kusar, D. Svetin, S. Brazovskii, and D. Mihailovic, *Science* **344**, 177 (2014).
- [16] S. Beaulieu, S. Dong, N. Tancogne-Dejean, M. Dendzik, T. Pincelli, J. Maklar, R. P. Xian, M. A. Sentef, M. Wolf, A. Rubio *et al.*, *Sci. Adv.* **7**, eabd9275 (2021).
- [17] D. R. Baykushcheva, H. Jang, A. A. Husain, S. Lee, S. F. R. TenHuisen, P. Zhou, S. Park, H. Kim, J. K. Kim, H. D. Kim, M. Kim, S. Y. Park, P. Abbamonte, B. J. Kim, G. D. Gu, Y. Wang, and M. Mitrano, *Phys. Rev. X* **12**, 011013 (2022).
- [18] J. A. Wilson, F. Di Salvo, and S. Mahajan, *Adv. Phys.* **24**, 117 (1975).
- [19] C. Scruby, P. Williams, and G. Parry, *Philos. Mag.* **31**, 255 (1975).
- [20] N. Smith, S. Kevan, and F. DiSalvo, *J. Phys. C* **18**, 3175 (1985).
- [21] F. Zwick, H. Berger, I. Vobornik, G. Margaritondo, L. Forró, C. Beeli, M. Onellion, G. Panaccione, A. Taleb-Ibrahimi, and M. Grioni, *Phys. Rev. Lett.* **81**, 1058 (1998).
- [22] J.-J. Kim, W. Yamaguchi, T. Hasegawa, and K. Kitazawa, *Phys. Rev. Lett.* **73**, 2103 (1994).
- [23] L. Perfetti, T. A. Gloor, F. Mila, H. Berger, and M. Grioni, *Phys. Rev. B* **71**, 153101 (2005).
- [24] M. Ligges, I. Avigo, D. Golez, H. U. R. Strand, Y. Beyazit, K. Hanff, F. Diekmann, L. Stojchevska, M. Kallane, P. Zhou, K. Rossnagel, M. Eckstein, P. Werner, and U. Bovensiepen, *Phys. Rev. Lett.* **120**, 166401 (2018).
- [25] P. Fazekas and E. Tosatti, *Philos. Mag. B* **39**, 229 (1979).
- [26] B. Sipos, A. F. Kusmartseva, A. Akrap, H. Berger, L. Forró, and E. Tutiš, *Nat. Mater.* **7**, 960 (2008).
- [27] K. T. Law and P. A. Lee, *Proc. Natl. Acad. Sci. USA* **114**, 6996 (2017).
- [28] M. Klanjšek, A. Zorko, R. Žitko, J. Mravlje, Z. Jagličić, P. K. Biswas, P. Prelovšek, D. Mihailovic, and D. Arčon, *Nat. Phys.* **13**, 1130 (2017).
- [29] A. S. Nганкеу, S. K. Mahatha, K. Guilloy, M. Bianchi, C. E. Sanders, K. Hanff, K. Rossnagel, J. A. Miwa, C. Breth Nielsen, M. Bremholm, and P. Hofmann, *Phys. Rev. B* **96**, 195147 (2017).
- [30] T. Ritschel, H. Berger, and J. Geck, *Phys. Rev. B* **98**, 195134 (2018).
- [31] Y. Wang, W. Yao, Z. Xin, T. Han, Z. Wang, L. Chen, C. Cai, Y. Li, and Y. Zhang, *Nat. Commun.* **11**, 4215 (2020).
- [32] P. Darancet, A. J. Millis, and C. A. Marianetti, *Phys. Rev. B* **90**, 045134 (2014).
- [33] T. Ritschel, J. Trinckauf, K. Koepernik, B. Büchner, M. v. Zimmermann, H. Berger, Y. Joe, P. Abbamonte, and J. Geck, *Nat. Phys.* **11**, 328 (2015).
- [34] C. Butler, M. Yoshida, T. Hanaguri, and Y. Iwasa, *Nat. Commun.* **11**, 2477 (2020).
- [35] Q. Stahl, M. Kusch, F. Heinsch, G. Garbarino, N. Kretzschmar, K. Hanff, K. Rossnagel, J. Geck, and T. Ritschel, *Nat. Commun.* **11**, 1247 (2020).
- [36] S.-H. Lee, J. S. Goh, and D. Cho, *Phys. Rev. Lett.* **122**, 106404 (2019).
- [37] J. Lee, K.-H. Jin, and H. W. Yeom, *Phys. Rev. Lett.* **126**, 196405 (2021).
- [38] C. Wen, J. Gao, Y. Xie, Q. Zhang, P. Kong, J. Wang, Y. Jiang, X. Luo, J. Li, W. Lu *et al.*, *Phys. Rev. Lett.* **126**, 256402 (2021).
- [39] F. Petocchi, C. W. Nicholson, B. Salzmänn, D. Pasquier, O. V. Yazyev, C. Monney, and P. Werner, *Phys. Rev. Lett.* **129**, 016402 (2022).
- [40] C. W. Nicholson, F. Petocchi, B. Salzmänn, C. Witteveen, M. Rumo, G. Kremer, F. O. von Rohr, P. Werner, and C. Monney, *arXiv:2204.05598*.
- [41] L. Perfetti, P. A. Loukakos, M. Lisowski, U. Bovensiepen, H. Berger, S. Biermann, P. S. Cornaglia, A. Georges, and M. Wolf, *Phys. Rev. Lett.* **97**, 067402 (2006).
- [42] L. Perfetti, P. A. Loukakos, M. Lisowski, U. Bovensiepen, M. Wolf, H. Berger, S. Biermann, and A. Georges, *New J. Phys.* **10**, 053019 (2008).
- [43] J. C. Petersen, S. Kaiser, N. Dean, A. Simoncig, H. Y. Liu, A. L. Cavalieri, C. Cacho, I. C. E. Turcu, E. Springate, F. Frassetto, L. Poletto, S. S. Dhesi, H. Berger, and A. Cavalleri, *Phys. Rev. Lett.* **107**, 177402 (2011).
- [44] C. Sohr, A. Stange, M. Bauer, and K. Rossnagel, *Faraday Discuss.* **171**, 243 (2014).
- [45] I. Avigo, I. Vaskivskiy, M. Ligges, M. Kalläne, K. Rossnagel, L. Stojchevska, D. Mihailović, and U. Bovensiepen, *Proc. SPIE* 9931, 99313V (2016).
- [46] I. Avigo, P. Zhou, M. Kalläne, K. Rossnagel, U. Bovensiepen, and M. Ligges, *Appl. Sci.* **9**, 44 (2019).
- [47] A. Simoncig, M. Stupar, B. Ressel, T. Saha, P. Rebernik Ribic, and G. De Ninno, *Phys. Rev. B* **103**, 155120 (2021).
- [48] J. Maklar, S. Dong, J. Sarkar, Y. Gerasimenko, T. Pincelli, S. Beaulieu, P. Kirchmann, J. Sobota, S.-L. Yang, D. Leuenberger *et al.*, *arXiv:2206.03788*.

- [49] Q.-H. Ren, T. Suzuki, T. Kanai, J. Itatani, S. Shin, and K. Okazaki, [arXiv:2207.05232](https://arxiv.org/abs/2207.05232).
- [50] K. Rossnagel, *J. Phys.: Condens. Matter* **23**, 213001 (2011).
- [51] See Supplemental Material at <http://link.aps.org/supplemental/10.1103/PhysRevB.107.L121103> for additional information about the materials and methods.
- [52] J. Ravnik, M. Diego, Y. Gerasimenko, Y. Vaskivskiy, I. Vaskivskiy, T. Mertelj, J. Vodeb, and D. Mihailovic, *Nat. Commun.* **12**, 2323 (2021).
- [53] F. Y. Gao, Z. Zhang, Z. Sun, L. Ye, Y.-H. Cheng, Z.-J. Liu, J. G. Checkelsky, E. Baldini, and K. A. Nelson, *Sci. Adv.* **8**, eabp9076 (2022).
- [54] M. Eichberger, H. Schäfer, M. Krumova, M. Beyer, J. Demsar, H. Berger, G. Moriena, G. Sciaini, and R. Miller, *Nature (London)* **468**, 799 (2010).
- [55] G. Lantz, B. Mansart, D. Grieger, D. Boschetto, N. Nilforoushan, E. Papalazarou, N. Moisan, L. Perfetti, V. L. Jacques, L. Bolloc'h *et al.*, *Nat. Commun.* **8**, 13917 (2017).
- [56] L. Le Guyader, T. Chase, A. Reid, R. Li, D. Svetin, X. Shen, T. Vecchione, X. Wang, D. Mihailovic, and H. Dürr, *Struct. Dyn.* **4**, 044020 (2017).
- [57] W. Li and G. V. Naik, *Nano Lett.* **20**, 7868 (2020).